Small-polaron transport in the Zn-doped colossal-magnetoresistance materials $Fe_{1-x}Zn_xCr_2S_4$

Shouguo Wang
Institute of Solid State Physics, Academia Sinica, Hefei 230031, People's Republic of China and Structure Research Laboratory, University of Science and Technology of China, Hefei 230026, People's Republic of China

Kebin Li
Institute of Solid State Physics, Academia Sinica, Hefei 230031, People's Republic of China and Data Storage Institute, National University of Singapore, 119260, Singapore

Zhixiang Chen
Institute of Solid State Physics, Academia Sinica, Hefei 230031, People's Republic of China

Yuheng Zhang
Structure Research Laboratory, University of Science and Technology of China, Hefei 230026, People's Republic of China and Institute of Solid State Physics, Academia Sinica, Hefei 230031, People's Republic of China

(Received 1 June 1999)

The electrical resistivity, magnetization, thermoelectric power, and specific heat have been studied on a series of Zn-doped polycrystalline samples $Fe_{1-x}Zn_xCr_2S_4$ ($0 \leqslant x \leqslant 0.75$) with a spinel structure over a wide range of composition and temperature. The properties show a systematical change with substituting monovalent and nonmagnetic Zn for Fe. At high temperatures, a significant difference between the activation energy deduced from the electrical resistivity $\rho(T)$ and the thermopower $S(T)$, a characteristic of small polarons, is observed. The conductivity is dominated by hopping of small polarons. All of the experimental data can be well explained on the basis of the polaron model. At the same time, we discuss the origin of the colossal magnetoresistance effect in these kinds of compounds.

INTRODUCTION

Since the discovery of the colossal magnetoresistance (CMR) effect in perovskitelike manganites,[1] a great interest has been attracted to investigate these ferromagnetic compounds.[2,3] The electronic, magnetic, and transport properties in perovskitelike manganites $L_{1-x}R_xMnO_3$ (where L = La, Pr *et al.* and R = Ba, Ca, *et al.*) could be described by double exchange (DE) model qualitatively.[4,5] Mills, Littlewood, and Shraiman[5] have pointed out, however, that double exchange alone cannot account for the large resistivity drop below the Curie temperature T_C. They proposed that lattice-polaronic effects due to strong electron-phonon coupling (arising from a strong Jahn-Teller effect) should be involved. P. Dai *et al.*[6] found an experimental evidence for existence of the dynamic Jahn-Teller effect subsequently. In spite of the effort expended, there is still no consensus of the microscopic mechanism causing the conductivity and CMR effect in perovskite manganites. For example, in 1996, M. A. Subramanian *et al.*[7] found a CMR material: pyrochlore $Tl_2Mn_2O_7$. This compound has neither mixed valence for a double exchange magnetic interaction nor a Jahn-Teller cation such as Mn^{3+}. Subsequently, Ramirez, Cava, and Krajewski[8] have reported the existence of CMR effect in a class of materials—Cr-based chalcogenide spinels such as $FeCr_2S_4$, in which there does not exist the double exchange interaction.

AB_2S_4-type compounds (A = Fe, Zn, *et al.* and B = Cr, Co, *et al.*) have the spinel structure which is different from that of the perovskite manganites. A-site ion is divalent on the tetrahedral sites and B-site ion is trivalent on the octahederal sites.[9,10] There is no site exchanging between A atoms and B atoms, and there is no A mixed valence in this type of compounds such as $FeCr_2S_4$. The magnitude of MR [$MR = (\rho(0) - \rho(H))/\rho(0)$] in spinel compounds is smaller than that in perovskitelike compounds under the same conditions. For instance, MR of $FeCr_2S_4$ is less than 20% while MR of $La_{0.5}Ca_{0.5}MnO_3$ is as high as 90% in a magnetic field up to 6 T.[8,11] In order to probe the mysteries of great difference of CMR effect in these compounds, the transport mechanism in AB_2S_4-type compounds needs further to be studied. If magnetic scattering is central to the transport phenomena of the system, it would cause a change mostly in μ with little variation in n (where μ is the mobility of carriers).[12] R. J. Bouchard[13] has reported that the activation energy necessary for conduction in these compounds depends upon the influence of A-site ions. By substituting Zn ion for Fe ion, we can study the influence of A-site ions because Zn ion is monovalent and nonmagnetic. The x-ray-diffraction patterns indicate that all $Fe_{1-x}Zn_xCr_2S_4$ samples with different concentrations have a spinel structure without any other secondary or impurity phase. These results indicate that the replacement of Fe by Zn ions has hardly any influence on its lattice because of the identical ion size of Fe^{2+} and Zn^{2+}. In this paper, we report the transport properties and the origin of CMR effect in the spinel $Fe_{1-x}Zn_xCr_2S_4$ compounds in more depth based on the experimental data of

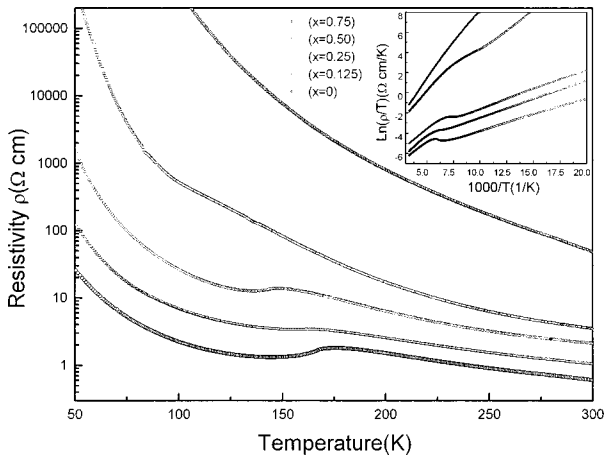

FIG. 1. The temperature dependence of resistivity for a series of $Fe_{1-x}Zn_xCr_2S_4$ samples with different Zn-doping concentrations. Inset: $\ln(\rho/T)$ versus $10^3/T$.

the electrical resistivity, magnetization, thermoelectric power (TEP), and specific heat.

EXPERIMENT

The polycrystalline samples of Zn-doped $Fe_{1-x}Zn_xCr_2S_4$ were prepared by the conventional solid-state synthesis method using high-purity iron powder, zinc powder, chromium powder, and sulfur powder. The powders were mixed in the stoichiometric ratios, ground thoroughly, and sealed into evacuated quartz tubes. The initial temperature was 450 °C, then it increased slowly with increment of 100 °C up to 850 °C over a period of one week, with intermediate grinding, and adding prompt sulfur powder. The resulting powder was densified by pressing into pellets under 20 atmosphere pressure with 10 mm diameter and 1 mm thickness. The pellets were fired in evacuated quartz tubes for 36 h at 900 °C and furnace cooled to room temperature. The structure and phase purity were checked by x-ray diffraction (XRD). The electrical resistivity was carried out using a conventional four-probe method. The temperature dependence of magnetization was measured by using a superconducting quantum interference device (SQUID) magnetometer. Specific-heat measurements were done in a standard ac calorimeter. The thermoelectric power (TEP) measurements were performed by suspending a sample between electrically isolated copper posts across which a variable temperature gradient was applied. Electrical contacts were achieved with silver paint.

RESULTS AND DISCUSSION

The temperature dependence of resistivity in zero magnetic field for all samples with respective doping concentrations is shown in Fig. 1. The curves show obviously that the resistivity increases rapidly with doping concentration increasing. For lower doping concentrations ($0 \leqslant x \leqslant 0.25$), the semiconductor-semiconductor transition has been observed. $\rho(T)$ in zero field increases rapidly, as the temperature is lowered, and reaches a maximum at peak temperature T_P, which is summarized in Table I. Below T_P, $\rho(T)$ falls abruptly in the narrow temperature region and then increases again as the temperature is further reduced. This behavior agrees with that reported by A. P. Ramirez.[8,10,13,14] At the doping level of $x=0.75$, $\rho(T)$ has a feature similar to that of a semiconductor in the whole temperature range measured. The sample with $x=0.50$ is a transition sample which has semiconductor-semiconductor transition but not obvious. With increasing the doping concentration the magnitude of T_P shifts to lower temperatures, and the transition becomes weaker. When the concentration x reaches 0.75 the transition disappears. The magnetization as a function of the temperature for all samples is plotted in Fig. 2. It can be seen that the samples with $x \leqslant 0.50$ undergo a transition from paramagnetic to ferromagnetic (PM-FM) phase. The temperature according to the maximum of $|dM/dT|$ is defined as the Curie temperature T_C, which is shown in Table I. With increasing x the value of T_C decreases, and when x reaches 0.75 PM-FM transition disappears.

TABLE I. Parameters of the various samples investigated in this work. x stands for the doping concentration. T_p is the temperature at which the resistivity reaches the maximum. T_C denotes the Curie temperature derived from the magnetization. $T_{S\text{-}H}$ is the temperature at which the specific heat maximum occurs at zero fields.

Sample No.	x	T_p (K)	T_C (K)	$T_{S\text{-}H}$ (K)
1	0	175.4	165.0	164.5
2	0.125	163.6	158.5	158.0
3	0.25	147.9	139.2	139.2
4	0.50	106.5	98.0	
5	0.75			

In order to gain an insight into the origin of the systematic resistivity change, one may recall that the electrical conductivity

$$\sigma = ne\mu, \tag{1}$$

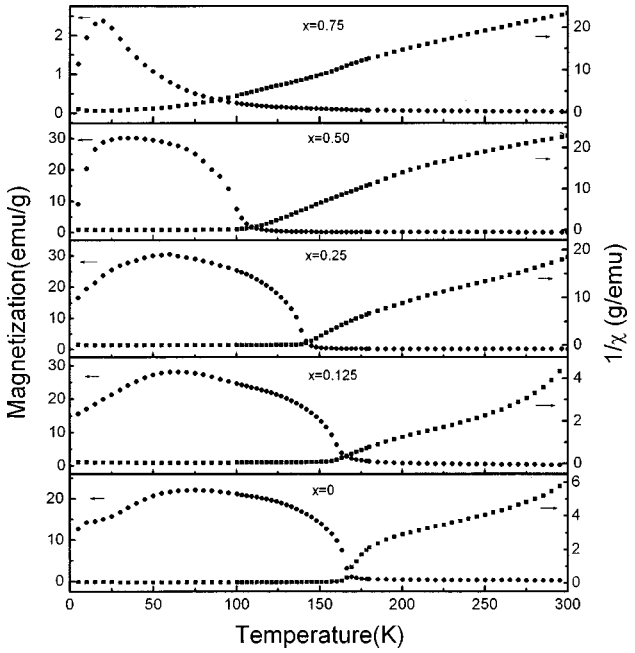

FIG. 2. The temperature-dependent magnetization and the inverse magnetic susceptibility in a magnetic field (1000 G) for samples with different concentrations.

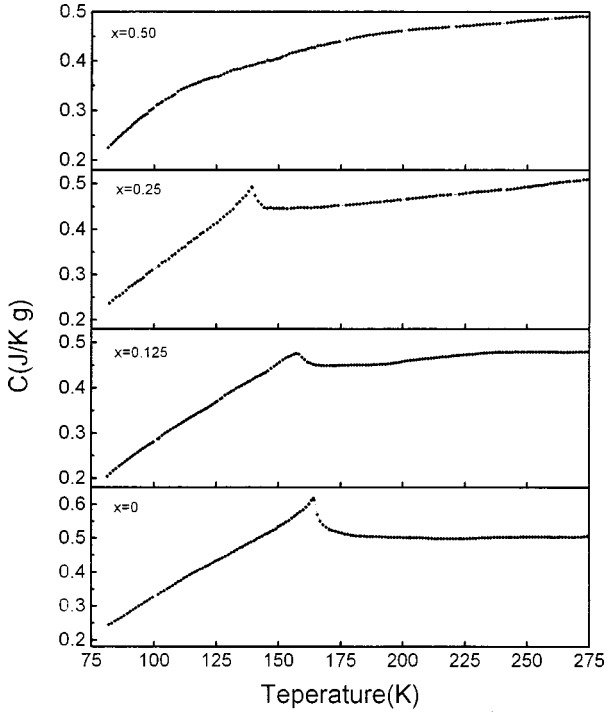

FIG. 3. Specific heat as a function of temperature for the samples with $x \leqslant 0.50$.

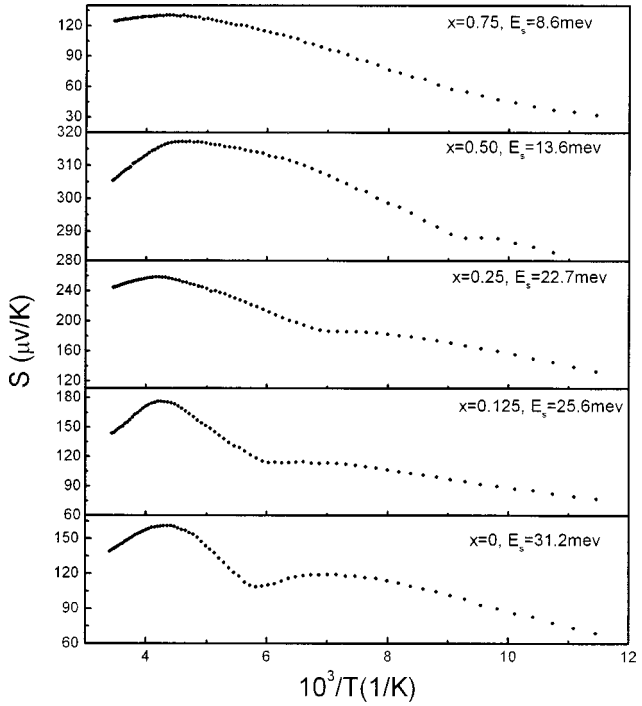

FIG. 4. The thermoelectric power (TEP) versus $10^3/T$ for all samples.

where n, e, and μ are the density, the electronic charge, and the mobility of carriers, respectively. Obviously, separate measurements of n and μ would be beneficial for a proper understanding of the transport mechanism in this kind of materials. We attempted to accomplish this purpose by simultaneously measuring the temperature dependence of resistivity $\rho(T)$ and specific heat $C(T)$. Figure 3 shows the temperature dependence of specific heat for four low-concentration samples. The samples with $x \geqslant 0.50$ have no peak in the curve, and the sample with $x=0.75$ is not shown in Fig. 3. The temperature $T_{\text{S-H}}$ at which the specific heat maximum occurs in zero field, is located at 164, 157, and 139 K, respectively, for the sample with $x \leqslant 0.25$. These values also coincide with the Curie temperatures T_C identified by measuring the magnetization. In order to get the relationship between the transport mechanism and the magnetic property, we calculated $d\rho/dT$ and found that $d\rho/dT$ shows a distinctive bell-shaped peak against temperature and the temperature at which $d\rho/dT$ reaches the maximum coincides with T_C. From Table I it can be seen clearly that $T_{\text{S-H}}=T_C<T_P$, and hence the specific heat peak is probably of magnetic origin.[12]

Figure 4 and the inset in Fig. 1 show the temperature dependence of thermopower $S(T)$ and $\ln(\rho/T)$ versus $1000/T$. For $T>T_C$, the temperature dependence of $\rho(T)$ and $S(T)$ can be well described by

$$\rho(T)=\rho_0 T \exp\left(\frac{E_\rho}{k_B T}\right), \tag{2}$$

and

$$S(T)=\frac{k_B}{e}\left(\alpha+\frac{E_S}{k_B T}\right), \tag{3}$$

respectively, where k_B is Boltzmann's constant, e is the electron's charge, and α is a sample-dependent constant. The values of E_ρ and E_s are given in Table II (where $E_{\rho H}$ denotes the activation energy at high temperatures, and $E_{\rho L}$ denotes the activation energy at low temperatures). In 1989, R. M. Kusters *et al.*[15] pointed out that activated semiconductorlike conductivity above T_C suggested the possibility of conduction by polarons in the paramagnetic regime. The significant difference between E_ρ and E_S, a characteristic of small polarons, indicates that the conventional band transport does not occur above T_C, but rather is the hallmark of small polaron hopping.[14–20]

A magnetic polaron consists of an electron which polarizes the magnetic moment of the ions around it, forming in effect a small ferromagnetic region, and the combination of

TABLE II. $E_{\rho H}$ and $E_{\rho L}$ denote the activation energy of above and below the Curie temperature, respectively. E_S shows the activation energy according to the TEP, respectively. W_H is the energy required to jump in a given direction. E_p is the binding energy of a polaron.

Sample No.	x	$E_{\rho H}$ (meV)	$E_{\rho L}$ (meV)	E_S (meV)	W_H/k_B (K)	E_p (meV)
1	0	67.1	28.5	31.2	417	71.8
2	0.125	69.0	32.1	25.6	503	86.8
3	0.25	73.1	34.3	22.7	584	100.8
4	0.50	102.1	75.6	13.6	1027	177.0
5	0.75	125.6		8.6	1358	234.0

the electron and its strain field is known as a polaron.[15] Magnetic polarons are localized as a consequence of magnetic interactions or at impurities, so that conduction proceeds via thermal hopping. Magnetic polarons, however, can only exist over a limited range of temperatures and magnetic fields. The paramagnetic state has been thought to be the environment of surviving of magnetic polarons. It can be seen clearly from Fig. 2 that the system is actually in paramagnetic state above T_C. Evidence of this kind magnetic polaron effect can also be obtained from the large short-range ferromagnetic contribution observed in the measurement of the magnetic susceptibility above T_C (Ref. 21). For the samples with PM-FM transition, $1/x$ deviates from the Curie-Weiss behavior well above T_C, which can be seen from Fig. 2. A more subtle effect of the electron-phonon interaction is the apparent increment in electron mass that occurs because the electron drags the heavy ion cores with it. In zero magnetic field, the formation of magnetic polarons will become impossible if the magnetic ions are ferromagnetically ordered.[14] That both $\ln\rho(T)$ and $S(T)$ deviate from linear behavior above T_C in zero field provides evidence of identical microscopic mechanisms, i.e., the onset of a long-range order, which can be supported by the temperature dependence of magnetization.

According to the small polaron model,[16,17] we can get Eqs. (4), (5), and (6):

$$\sigma(T)=\frac{A}{T}\exp\left(-\frac{\varepsilon_0+W_H-J}{k_BT}\right), \tag{4}$$

$$S(T)=\frac{K_B}{e}\left(\alpha+\frac{\varepsilon_0}{k_BT}\right), \tag{5}$$

$$E_P=2W_H, \tag{6}$$

where A is a sample-dependent constant, W_H is the energy required to jump in a given direction, J is the transfer integral, and E_P is the binding energy of a polaron, ε_0 is the energy difference between identical lattice distortions with and without the carrier, that is to say, it is the energy required to generate carriers. We compare the Eqs. (2) and (3) with Eqs. (4) and (5), and get the following relationships: $E_\rho\equiv\varepsilon_0+W_H-J$ and $E_S\equiv\varepsilon_0$, respectively. Assuming, as usual, that $J\ll W_H$ we note that the condition $T<W_H/k_B$ is satisfied, and we get the polaron binding energy shown in Table II.

According to the polaron model, the measured activation energy E_ρ is the sum of the activation energy needed for the creation of the carriers and activating the hopping of carriers, and E_S is the energy required to activate the hopping of carriers. Therefore the activation energy E_ρ is larger than E_S at the high-temperature range. When the temperature decreases to T_C, the system undergoes the transition from paramagnetic to ferromagnetic (PM-FM) phase. The onset of short-range ferromagnetic order leads to an abrupt expansion of polarons, resulting in the formation of metallic conductivity. The applied magnetic field promotes the onset of ferromagnetic order. As a consequence, the PM-FM transition occurs at higher temperatures. In this temperature range, which is the difference between the PM-FM transition temperatures in magnetic fields and in zero field, the carrier is polarons in zero magnetic field, but is delocalized carriers in applied magnetic fields at the same temperature, which leads to the abrupt decrease of conductivity. This is the origin of CMR in this kind of compounds.

The doping of Zn will decrease the bandwidth of the polaron band gap, so that the energy E_s decreases. At the same time, the binding energy becomes larger as can be seen from Table II, and thus the resistivity increases. From Fig. 2 we can see that the onset of long-range magnetic order occurs around the Curie temperature T_C. The abrupt drop in both $\rho(T)$ and $S(T)$ near T_C is fully consistent with carrier delocalization due to the onset of long-range magnetic order.

In the plot of $\ln\rho(T)$ versus $10^3/T$ shown in the inset of Fig. 1 a break occurs, which indicates that the different mechanisms are operative in different regions of the curve for the semiconductor materials.[13] When the onset of long-range magnetic order occurs, the polaron begins to delocalize, and the formation of magnetic polarons will become impossible if the magnetic ions are magnetically ordered.[15,16] Hence, we can conclude that the conductivity at the high-temperature range is dominated by hopping of localized magnetic polarons, and the conductivity at the low-temperature range by thermal-activated hopping of carriers like semiconductors. At high temperatures one would not expect that the magnetic correlation range grows to a large extent. However, once the system enters the polaron band regime from the high-temperature side, the magnetic correlation would develop rapidly, giving rise to the specific heat peak below T_P as was mentioned above. For the sample $x=0.75$, there is no transition from semiconductor to metal due to the larger doping concentration which inhibits the onset of long-range magnetic order.

At very low temperatures, the sample resistance begins to increase again and the magnetization begins to decrease. This may be the onset of some form of localization due to antiferromagnetic ordering of the Cr^{3+} ions, and this temperature range is under investigation at present.

CONCLUSION

In summary, the transport properties of Zn-doped $Fe_{1-x}Zn_xCr_2S_4$ system have been studied carefully by using the resistivity, TEP, specific heat, and magnetization. This kind of materials show fascinating properties in many aspects. We find that the specific heat is of magnetic origin, and the resistivity in the paramagnetic phase has an activated form, whereas the activation energy is not compatible with the formation of the TEP. The large difference between the activation energies, deduced from the electrical resistivity $\rho(T)$ and thermopower $S(T)$ respectively, is the characteristic of small polarons. The conductivity at the high-temperature range is dominated by hopping of localized magnetic polarons, and the conductivity at the low-

temperature range by thermal-activated hopping of carriers. We also point out the origin of CMR in these kinds of compounds. This systematical study would shed light on the physic origin study of this kind of CMR materials and open up a vast range of material for the further exploration and exploitation of CMR effect.

ACKNOWLEDGMENTS

One of the authors, S. G. Wang, greatly appreciates the help of Professor Y. P. Sun for measuring the magnetic properties by means of SQUID. This work was supported by the Chinese Academy of Sciences under Contract No. KJ951-A1-401.

[1] R. von Helmolt, J. Wecker, B. Holzapfel, L. Schultz, and K. Samwer, Phys. Rev. Lett. **71**, 2331 (1993).
[2] A. J. Mills, B. I. Shraiman, and R. Mueller, Phys. Rev. Lett. **77**, 175 (1996).
[3] H. Roder, Jun Zhang, and A. R. Bishop, Phys. Rev. Lett. **76**, 1356 (1996).
[4] C. Zener, Phys. Rev. **82**, 403 (1951).
[5] A. J. Mills, P. B. Littlewood, and B. I. Shraiman, Phys. Rev. Lett. **74**, 5144 (1996).
[6] P. Dai, Jiandi Zhang, H. A. Mook, S.-H. Liou, P. A. Dowben, and E. W. Plummer, Phys. Rev. B **54**, R3694 (1996).
[7] M. A. Subramanian, B. H. Toby, A. P. Ramirez, W. J. Marshall, A. W. Sleight, and G. H. Kwei, Science **273**, 81 (1996).
[8] A. P. Ramirez, R. J. Cava, and J. Krajewski, Nature (London) **386**, 156 (1997).
[9] P. F. Bongers, C. Haas, A. M. J. G. Van Run, and G. Zanmarchi, J. Appl. Phys. **40**, 958 (1969).
[10] Zhiwen Chen, Shun Tan, Zhaorong Yang, and Yuheng Zhang, Phys. Rev. B **59**, 11 172 (1999).
[11] R. Mahendiran, R. Mahesh, A. K. Raychaudhuri, and C. N. R. Rao, Solid State Commun. **94**, 515 (1995).
[12] Soo Hyun Park, Yoon-Hee Jeong, Ki-Bong Lee, and S. J. Kwon, Phys. Rev. B **56**, 67 (1997).
[13] R. J. Bouchard, P. A. Russo, and A. Wold, Inorg. Chem. **4**, 685 (1965).
[14] T. Watanabe, Solid State Commun. **12**, 355 (1973).
[15] R. M. Kusters, J. Singleton, D. A. Keen, R. Mcgreevy, and W. Hayes, Physica B **155**, 362 (1989).
[16] M. F. Hundely and J. J. Neumeier, Phys. Rev. B **55**, 11 511 (1997).
[17] M. Jaime, M. B. Salamon, K. Pettit, M. Rubinstein, R. E. Treece, J. S. Horwitz, and D. B. Chrisey, Appl. Phys. Lett. **68**, 1576 (1996).
[18] M. Jaime, M. B. Salamon, M. Rubinstein, R. E. Treece, J. S. Horwitz, and D. B. Chrisey, Phys. Rev. B **54**, 11 914 (1996).
[19] T. T. M. Palstra, A. P. Ramirez, S.-W. Cheong, B. R. Zegarski, P. Schiffer, and J. Zaanen, Phys. Rev. B **56**, 5104 (1997).
[20] Michael Ziese and Chatchai Srinitiwarawong, Phys. Rev. B **58**, 11 519 (1998).
[21] J. M. De Teresa, M. R. Ibarra, P. A. Algarabel, C. Ritter, C. Marqulna, J. Blasco, J. Garcia, A. del Moral, and Z. Arnold, Nature (London) **386**, 256 (1997).